

See discussions, stats, and author profiles for this publication at:
<https://www.researchgate.net/publication/229966211>

Impact of Low-Dosage Inhibitors on Clathrate Hydrate Stability

ARTICLE *in* MACROMOLECULAR SYMPOSIA · JANUARY 2010

DOI: 10.1002/masy.201050124

CITATIONS

8

READS

40

5 AUTHORS, INCLUDING:



Tatyana Kuznetsova

University of Bergen

59 PUBLICATIONS 688 CITATIONS

SEE PROFILE



Bjørn Kvamme

University of Bergen

364 PUBLICATIONS 1,650

CITATIONS

SEE PROFILE

Impact of Low-Dosage Inhibitors on Clathrate Hydrate Stability

Tatiana Kuznetsova,^{*1} Alla Sapronova,² Bjørn Kvamme,¹ Klaus Johannsen,² Jarle Haug¹

Summary: Development of more capable low-dosage hydrate inhibitors (LDHI) is of crucial importance to oil and gas industry. Those efforts have been severely hindered so far by lack of clear understanding of molecular-level mechanisms, both thermodynamic and kinetic, which make certain chemical compounds into efficient inhibitors. An accurate representation of intermolecular potentials between polymeric low dosage inhibitors and hydrate-water-gas surfaces is essential for modelling systems containing these components.

A two-stage computational study was undertaken of two proven LDHIs, polyvinylpyrrolidone (PVP) and polyvinylcaprolactam (PVCap), in aqueous solutions under various conditions. We have first carried out *ab initio* density functional theory (DFT) calculations for PVP and PVCap polymers with molecular weight spanning from monomers to polymeric chains. Molecular dynamics were then employed to investigate thermodynamic and kinetic processes that affect hydrate nucleation and growth. Comparison with experiments has also shown that calculated potential is able to mimic the characteristic behaviour of methane hydrate and PVP complexes.

Keywords: *ab initio*; clathrate hydrates of natural gases; low-dosage inhibitors; molecular dynamics

Introduction

Clathrate hydrates of natural gases are ice-like formations composed of guest gas molecules encaged by water molecules. A large number of cases are capable of forming hydrates; they range from light hydrocarbons to refrigerants to sour gases like carbon dioxide and hydrogen sulphate.^[1] Under conditions relevant for oil and gas production and transport in colder climes, clathrate hydrates can easily form in the pipelines and production equipment. This has long been a problem for the petroleum industry. Traditionally, hydrate formation is prevented by injecting large

quantities (up to 40 wt%) of alcohols and glycols into production streams. The cost of chemicals and cleanup has spurred on an interest in so-called “kinetic” or low-dosage inhibitors able to slow down the process of hydrate formation rather than make it impossible.

Testing of potential kinetic inhibitors involves numerous costly and time-consuming experiments at high pressures. If numerical simulations can be used to cull the list of experimental candidates, computers may prove to be an invaluable research tool. Since it is not currently feasible to reproduce the whole process of hydrate nucleation and growth in numerical simulations, measurement and comparison of the efficiency of potential inhibitor compounds implies identifying the inhibition mechanism/mechanisms. Numerical simulations are then run to see how well the inhibitor candidates can

¹ Department of Physics and Technology, University of Bergen, Allég. 55, 5007, Bergen, Norway
Fax: (+47)55589440;

E-mail: tatiana.kuznetsova@ift.uib.no

² Bergen Center for Computational Science

perform tasks associated with different inhibition steps.

The fundamental mechanisms of kinetic hydrate inhibition are still poorly understood; with several hypotheses suggested by different groups. A group at the Massachusetts Institute of Technology (MIT) proposed the following 2-step mechanism for kinetic inhibition^[2]:

- (a) inhibitor molecules disrupt the local organization of the water and guest molecules, increasing the barrier to nucleation and nuclei propagation;
- (b) once nucleation occurs, the inhibitor binds to the surface of hydrate nanocrystal and retards growth along the bound growth plane. The group of Prof. M. Rodger at the University of Warwick showed that PVP induces dissolution of small hydrate clusters without any direct contact between the additive and the hydrate surface. They hypothesized that PVP increases the interfacial surface energy without adsorbing onto hydrate surface, thus disrupting step (b) of MIT hypothesis.^[3–5]

Prof. B. Kvamme and co-workers from the University of Bergen,^[6,7] while agreeing in general with step (a) of the MIT hypothesis and numerical findings of the University of Warwick, have put forward an inhibition mechanism emphasizing the role of kinetic factors.

We assume that PVP and similar LDHI will form a layer between the water and the gas phase. Hydrate formers will have to traverse this layer before any hydrate formation can start. The diffusion of gas through the polymer phase is thus suggested as the limiting factor in the hydrate formation process.

Methodology

Quantum Mechanical Calculation

An accurate representation of intermolecular potentials for multi-component system modelling is essential. Whenever standard force fields used for large scale

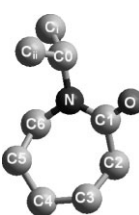
molecular dynamics simulations do not yield reasonable results, quantum mechanical calculations must be employed. In this work, numerical potentials of PVP and PVCap polymers were revised by running series of non-empirical calculations as a preliminary step. For the correct prediction, density functional theory (DFT) methods have been chosen. All problems encountered by MP2 schemes, such as accounting correctly for van der Waals and hydrophobic interactions, are heightened for multi-component and multiphase systems.

All calculations were done using GAUSSIAN 03,^[14] with initial molecular models built in HyperChem Professional 8.05.^[15] A set of static calculations (local geometry optimization) were done for a single monomer, dimer, and tetramer of PVP/PVCap units in gas and water phases. Bond lengths and molecular orientation were allowed to relax to avoid including unrealistic strain or electrostatic energy from displaced atoms.

Because of computer resources necessary, after optimizing geometry at *at initio* Hartree Fock level, each model was calculated at B3LYP with 6-311G(d) basis set known to be sufficient for obtaining numerical potentials.^[16] Calculations were done on IBM e1350 Linux cluster. Geometry optimization with DFT took around 0.5 hour per step, with about 20 steps needed to obtain a converged result for the geometry of a single PVCap monomer.

Table 1.

Calculated atomic charges for a PVCap monomer in gas and water phases; carbon atoms labelled as shown, for Hartree Fock and B3LYP theory levels with 6-311G basis set.

		HF/6-311G		B3LYP/6-311G	
		Gas	Water	Gas	Water
		phase	phase	phase	phase
	N	−0.68	−0.66	−0.52	−0.49
	C6	−0.13	−0.07	−0.11	−0.09
	C5	−0.32	−0.11	−0.32	−0.15
	C4	−0.31	−0.17	−0.33	−0.15
	C3	−0.32	−0.09	−0.32	−0.12
	C2	−0.42	−0.15	−0.33	−0.13
	C1	0.76	0.27	0.18	0.17
	O	−0.62	−0.41	−0.41	−0.33
	Co	0.03	0.05	0.03	0.05
	Cl/Cii	−0.48	−0.16	−0.48	−0.16

Optimization yielded Mulliken atomic charges and atomic charges with hydrogens summed into heavier atoms. It can be utilized further as parameters for consequent molecular dynamic simulations. Similar set of calculations were also performed for PVCap dimers. The change-over from monomer to dimer has revealed somewhat puzzling attenuation of the nitrogen's partial charge. While it remained consistently highly negative in both gas and water phase in the monomer, the partial charge dropped almost to zero in dimer and tetramer (-0.04 on average).

MD Simulation Details

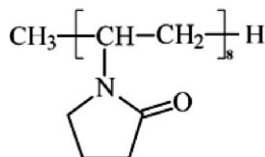
NVT molecular dynamics utilized a modified and extended version of the md43 package originally by Lyubartsev and Laaksonen.^[8] Periodic Boundary Conditions were applied in all three directions. Temperature was controlled by the Nosè - Hoover thermostat. Molecular interactions were modelled using a combination of Lennard-Jones potentials for short-range forces and Coulombic forces for interactions between partial charges. Ewald summation was applied for treatment of long-range electrostatic interactions.

Simple-point-charge-extended (SPC/E) model^[9] was used for water, both in liquid phase and hydrate crystal. Oxygen-hydrogen bond length was fixed via SHAKE-type constraint, with the spring force restraining the angle around 109.47° . One-site OPLS model used for methane.^[10]

Lingering doubts concerning the applicability of *ab initio* partial charges (see the previous section) made us reuse PVP force field parameters successfully used in our earlier investigations.^[7,11] Details on the PVP octamer force field and geometry can be found elsewhere.^[11]

PVP octamers consisted of eight PVP monomers with an additional CH_3 group and hydrogen atom at the ends as shown schematically below. Atomic groups were connected by fixed-length bonds. Additional fixed length bonds were used to replace angles in the ring and in the backbone. Finally, MM3-type torsions^[12]

were used for dihedral angles in the backbone. The ring was almost flat, and the backbone configuration initially all *trans*. MD snapshots and RDF calculations presented in this work were made by means of Visual Molecular Dynamics package of Humphrey *et al.*^[13]



Three Building Blocks

Several cells were created as basis for the simulations. Each of them contained different combination of five building boxes as described below. At this stage, all molecules are considered rigid. Temperature was set to 1°C , and the time step used for equilibration was 1 fs for all the boxes. At the beginning of equilibration, velocities were assigned according to the Maxwell distribution. The initial orientations of molecules were chosen at random, and the box systems equilibrated for 0.5–1.0 million time steps.

Box 1, pure liquid water: 3096 water molecules placed at fcc lattice vertices in a cell measuring $48.12 \text{ \AA} \times 48.12 \text{ \AA} \times 40.00 \text{ \AA}$.

Box 2, water plus PVP: 3093 water molecules and 3 PVP octamers were placed in fcc arrangement in a cell identical to the one above. Water molecules within $0.6\text{--}0.8 \text{ \AA}$ of PVP octamers were then manually removed. The other molecular forces were scaled. The final box consisted of 2948 water molecules and 3 PVP octamers resulting in a density equal to that of pure water.

Box 3, pure methane: cell measuring $48.12 \text{ \AA} \times 48.12 \text{ \AA} \times 40.00 \text{ \AA}$ created by placing 830 methane molecules in a fcc lattice.

Box 4: 827 methane and 3 PVP octamer molecules were arranged on an fcc lattice in a cell with the same dimension as Box 3. Methane molecules within $0.6\text{--}0.8 \text{ \AA}$ of the octamers were removed manually. Other molecular forces due to severe overlapping were scaled. The final cell consisted of 800 methane molecules and 3 PVP octamers.

Box 5, fully occupied methane hydrate: $4 \times 4 \times 4$ unit cells of structure I

hydrate were created from 2944 water and 388 methane molecules basing on known crystallographic coordinates of water in this hydrate. Methane molecules occupied the centers of all cavities. Translational movement for the methane molecules were then allowed, with water engaged initially only in rotational motions to prevent rapid melting of hydrate.

Results and Discussion

PVP Octamers in Liquid Water + Methane

Boxes 2 and 3 used as building blocks. The initial configuration consisted of liquid

water phase containing three PVP octamers, and a second phase of dense methane gas. The PVP octamers were positioned well within the water phase bulk. Simulations were run for approximately 20 ns with time steps of 0.5 femtosecond. All of the octamers eventually drifted towards the interface. Figure 1 shows a series of snapshots depicting the progress of the simulation.

As seen in Figure 1, two octamers initially placed close to the water interfaces moved towards the nearest interface rather quickly and then positioned themselves on the surface with their backbones facing the

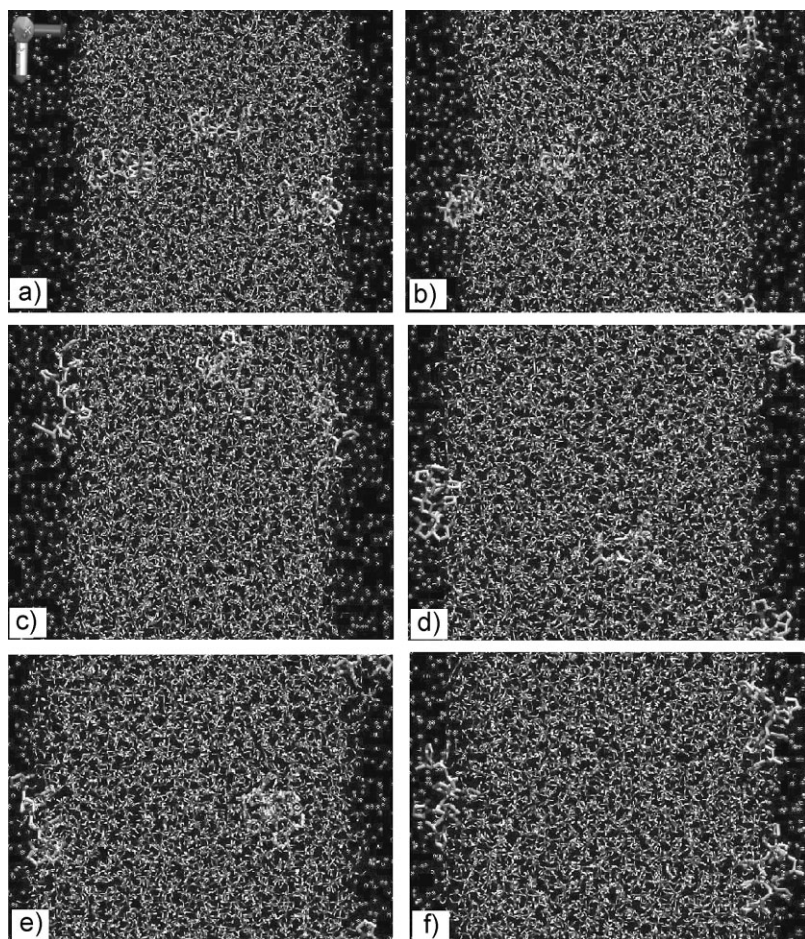


Figure 1.

The progress of PVP octamers towards water-methane interface in the system where PVPs start in water bulk: a) 0 ns, b) 4 ns, c) 8 ns, d) 15 ns, e) 16 ns, f) 20 ns. Oxygen is red; hydrogen-white, carbon-cyan; nitrogen-dark blue.

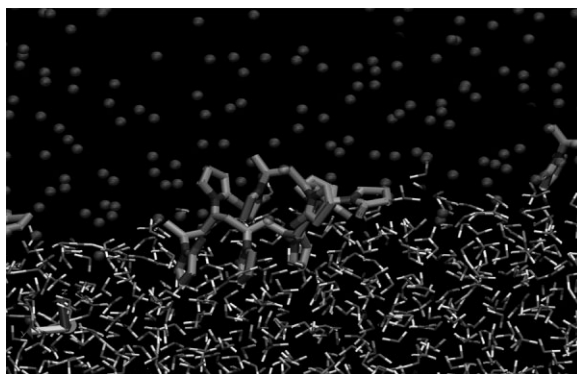


Figure 2.

PVP octamer with the longest residence time on the surface. Snapshot taken at the end of simulation, 20 ns.

methane phase. PVP octamer that started in the water bulk, took considerably longer to reach the interface (about 16 ns). Also, when it arrived, the octamer chose an area far away from the previous surfaced octamer.

A characteristic snapshot of the first PVP to reach the surface is shown in Figure 2. Three of the polymer rings are aligned normally to the interface and partially immersed in water, separating PVP backbone from the water surface. On average, 4+ hydrogen bonds were formed between each PVP polymer and liquid water. The number of hydrogen bonds was estimated using a script within the VMD package^[13] that used a rather conservative cutoff distance of 3.1 Å and angle cutoff of 25 degrees. The snapshot in

Figure 3 shows a PVP octamer with 5 hydrogen bonds anchoring it to the water surface.

Both visual inspection and radial distribution functions (RDF) showed that the PVP backbone prefers a location quite a distance away from the water surface. The RDF demonstrated no features indicative of short range order.

Radial distribution functions for PVP-oxygen and water-oxygen in Figure 4 indicate an existence of additional short-range structuring of water in proximity of PVP. In contrast with the RDF for oxygen–oxygen in water (same figure), the PVP RDF has 4 peaks (overlapping and thus not clearly visible in the picture). The water–water RDF was estimated using a pure water system also at 274 K, with periodic

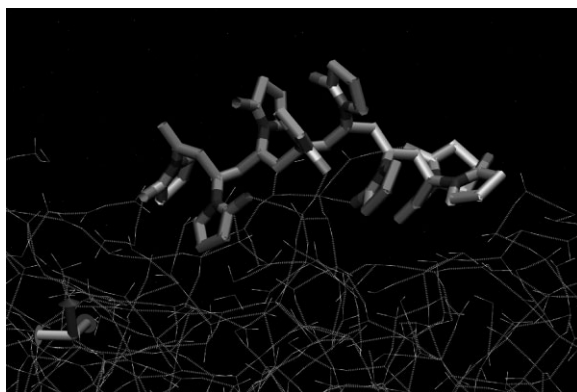


Figure 3.

Five hydrogen bonds formed between PVP oxygen and water surface.

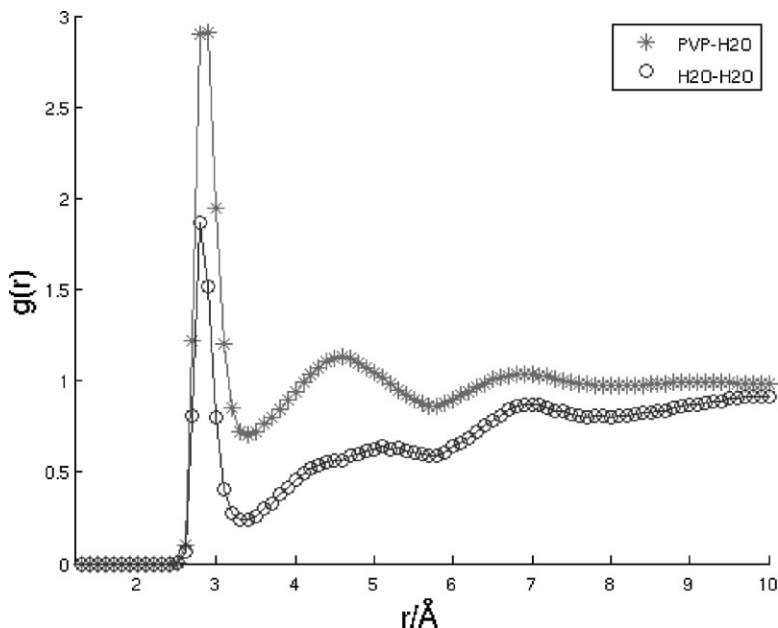


Figure 4.

RDFs for PVP oxygen and water oxygen (blue open circles). Analogous RDFs for oxygen – oxygen in pure water (red asterisks).

boundary conditions applied in all directions. Same VMD plug-in was used, thus allowing for unbiased comparison.

Results presented above suggest that though PVP rings disrupt slightly the hydrogen-bond structure, PVP will still bind to the water surface via oxygen. Moreover, with PVPs presenting attractive hydrogen-binding sites for liquid water molecules, water might prefer to interact with PVP rather than build hydrate structures. These findings are supported further by comparison of PVP oxygen – water hydrogen and the water oxygen – water hydrogen RDFs presented in Figure 5.

Diffusivity of a water molecule close to a PVP octamer immersed in water was compared to the diffusivity of water molecules in bulk liquid. First, we followed a randomly picked a randomly picked molecule from bulk water for 0.3 ns. This was done late in the simulation when all PVP octamers had diffused to the water-methane interface.

For comparison, we inspected a similar trajectory for a water molecule originally

placed close to a PVP octamer. This was done earlier in the simulation when one of the PVP octamers was still immersed in the water phase. Though the overall displacement over the period of 0.3 ns was similar for the two molecules, the distance travelled by the “bulk” molecule is about 10–15% longer. Closer analysis of the trajectory for the water molecule initially placed close to PVP reveals that the molecule was “pinned down” at the start of the trajectory. This might indicate reduced mobility of water molecules close to the PVP octamer and thus hindered restructuring necessary for hydrate formation.

PVP Octamers in Methane + Liquid Water

Boxes 4 and 1 were used. The initial configuration comprised of three PVP octamers placed well inside a dense methane phase, with the methane slab side-by-side and with the second phase consisting of liquid water. To analyze the behavior of PVP octamers on the methane gas – liquid water interface, the octamers were initially placed in the methane phase

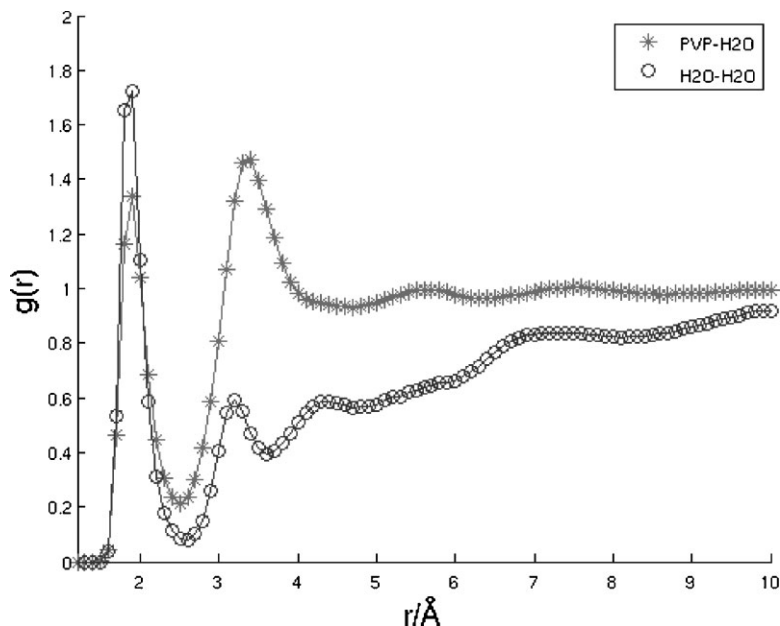


Figure 5.

RDFs for PVP oxygen and water hydrogen (open blue circles). Analogous RDFs for oxygen – oxygen in pure water (red asterisks).

and expected to diffuse into the interface. The simulations were run for approximately 12 ns with the time step of 0.5 fs. PVP octamers rapidly diffused to the interface and remained there, continuing to move alongside the surface. PVP backbones appeared to be aligned above the water surface with the rings mostly pointing out into methane. It is our belief that this system reached a metastable rather than truly stable state.

Structure I hydrate + PVP Octamers in Water

Boxes 2 and 5 used. The initial configuration consisted of $4 \times 4 \times 4$ units of fully occupied structure I methane hydrate with its {110} crystallographic plane facing aqueous phase containing three PVP octamers. This system was originally created to obtain insights into the interaction of PVP with the hydrate surface. To keep hydrates from melting has proven difficult in previous simulations. Thus, a relatively large hydrate crystal was created, hoping this would give a stable hydrate phase. Nevertheless, the

hydrate phase melted within 4 ns, creating methane-rich liquid water phase. A methane bubble then formed and one of the PVP octamers settled on the interface between bubble and liquid water. The simulation was run for approximately 7 ns with a time step of 1 femtosecond. Several snapshots from the simulation run are shown in Figure 6.

No extensive analysis of the PVP interaction with the hydrate surface is presented due to hydrate meltdown. Though the hydrate started melting immediately, its structures persisted to a large degree until 4 ns into the run. This would give the PVP octamers an ample opportunity to travel towards the hydrate surface, if attracted to it, given the time taken for PVPs placed close to the water – methane surface in the earlier discussed PVP – methane + water system. However, no sign of such an attraction has been seen. This supports the hypothesis of the University of Warwick group,^[3–5] that PVP inhibits hydrate nucleation without actually coming in contact with the hydrate-nucleate surface.

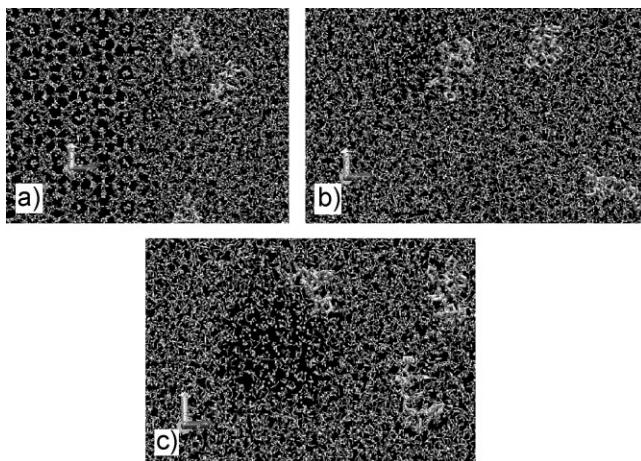


Figure 6.

Formation of methane bubble from melted hydrate, and its interaction with PVP octamers. a) 1 ns, initial configuration, b) 3 ns, melted hydrate, methane bubble has started to form, c) 7 ns, methane bubble developed and interacting with PVP octamer.

Experimental Study

A sample of PVP polymer in powder form, Luvitec K17, was purchased from BASF. This powder was dissolved in water at concentrations ranging from 0.5 wt% to 15 wt%. The polymer appeared uniformly dissolved in the water at all concentrations, with the solution turning yellow at the higher concentrations. Samples were then cooled to 4 °C and allowed to settle for 48 hours. On visual inspection, no phase separation was present. The solutions showed no indication of a concentration gradient. The solutions appeared completely uniform on visual inspection.

To investigate the homogeneity of the PVP solution further, nonpolar fluid decane was inserted in the earlier prepared PVP solutions. Decane formed a clear phase on top of the PVP solution. The solutions were then stored at 4 °C environment for weeks with regular inspections. No signs of phase separation or concentration gradient in the PVP solution could be seen, it appeared perfectly homogenous on visual inspection for all concentrations.

Both the present experimental work and datasheets from PVP manufacturers thus show that PVP is soluble in water from 0 to

15 wt%. If the theory presented by the University of Bergen group is correct, then methane diffusion through a separate macroscopic PVP layer is indeed the limiting factor for hydrate formation. Our atomistic studies would indicate that the formed layer is very thin and invisible to the naked eye. Additional experimental investigation, perhaps employing light scattering techniques, is therefore necessary.

Conclusions

Thus, we see the behaviour of “PVP in water – hydrate structure I” system as supporting the theoretical and modelling findings of the Warwick group who reported PVP inhibiting hydrate formation without approaching hydrate nucleus.

PVP octamers in “PVP in methane – liquid water” system rapidly diffused to the methane-water interface and stayed there, moving alongside the surface throughout the simulation. PVP backbones were aligned along the water surface, with the majority of rings pointing towards the methane phase, somewhat counter intuitively.

“PVP in water – methane” system was the one coming closest to reproducing real

gas-water systems though it contradicted the findings in the PVP in methane – liquid water system where PVP backbones were oriented towards the water surface. We believe that the latter system exhibited a metastable PVP conformation in contrast to the “PVP in water – methane” system. PVP formed hydrogen bonds with the interfacial water, and thus might hinder water molecules from engaging in hydrate formation. Comparison of RDFs has also revealed additional structuring of water. This supports mechanism proposed by both the Warwick and MIT groups, that distortion of water structure in the vicinity of PVP will retard hydrate formation.

In all three simulated systems, PVP exhibited a strong attraction for the methane-water surface. An aqueous solution of PVP in contact with methane will have a surface covered with PVP. Moreover, PVPs rings extending into water will attract more PVP octamers and thus create a microscopic interface layer not visible on inspection. This layer would present an obstacle for hydrate formation since it is positioned between the hydrate formers. The mass transport through the layer will thus be an important restriction for hydrate formation and contribute to PVP's performance as kinetic hydrate inhibitor.

- [1] E. D. Sloan, “Clathrate Hydrates of Natural Gases”, (second ed), Marcel Dekker Inc., New York 1998.
- [2] B. J. Anderson, J. W. Tester, G. P. Borghi, B. L. Trout, *J.A.C.S.* **2005**, 127, 17852.
- [3] C. Moon, *Canadian Journal of Physics* **2003**, 81, 451.
- [4] C. Moon, R. W. Hawtin, et al. Nucleation and control of clathrate hydrates: insights from simulation. **2007**, 136, 367–382.
- [5] M. T. Storr, P. C. Taylor, J. P. Monfort, P. M. Rodger, *J. Am. Chem. Soc.* **2004**, 126, 1569.
- [6] B. Kvamme, T. Kuznetsova, K. K. Aasoldsen, *Journal of Molecular Graphics & Modelling* **2005**, 23, 524.
- [7] R. Åsnes, Master Sci. Thesis **2006**, “Prediction of hydrate kinetic inhibitors performance”, UiB.
- [8] A. P. Lyubartsev, A. Laaksonen, *Computer Physics Communications* **2000**, 128, 565.
- [9] H. J. C. Berendsen, *J Phys. Chem.* **1987**, 91, 6269.
- [10] W. L. Jorgensen, *J. Am. Chem. Soc.* **1984**, 106, 6638.
- [11] B. Kvamme, G. Huseby, O. K. Forrisdahl, *Mol. Phys.* **1997**, 90, 979.
- [12] W. L. Jorgensen, *J. Phys. Chem.* **1986**, 90, 1276.
- [13] W. Humphrey, A. Dalke, K. Schulten, *J. Molec. Graphics* **1996**, 14, 33.
- [14] Gaussian 03, M. J. Frisch, G. W. Trucks, H. B. Schlegel, G. E. Scuseria, M. A. Robb, J. R. Cheeseman, J. A. Montgomery, Jr., T. Vreven, K. N. Kudin, J. C. Burant, J. M. Millam, S. S. Iyengar, J. Tomasi, V. Barone, B. Mennucci, M. Cossi, G. Scalmani, N. Rega, G. A. Petersson, H. Nakatsuji, M. Hada, M. Ehara, K. Toyota, R. Fukuda, J. Hasegawa, M. Ishida, T. Nakajima, Y. Honda, O. Kitao, H. Nakai, M. Klene, X. Li, J. E. Knox, H. P. Hratchian, J. B. Cross, V. Bakken, C. Adamo, J. Jaramillo, R. Gomperts, R. E. Stratmann, O. Yazyev, A. J. Austin, R. Cammi, C. Pomelli, J. W. Ochterski, P. Y. Ayala, K. Morokuma, G. A. Voth, P. Salvador, J. J. Dannenberg, V. G. Zakrzewski, S. Dapprich, A. D. Daniels, M. C. Strain, O. Farkas, D. K. Malick, A. D. Rabuck, K. Raghavachari, J. B. Foresman, J. V. Ortiz, Q. Cui, A. G. Baboul, S. Clifford, J. Cioslowski, B. B. Stefanov, G. Liu, A. Liashenko, P. Piskorz, I. Komaromi, R. L. Martin, D. J. Fox, T. Keith, M. A. Al-Laham, C. Y. Peng, A. Nanayakkara, M. Challacombe, P. M. W. Gill, B. Johnson, W. Chen, M. W. Wong, C. Gonzalez, J. A. Pople, Gaussian, Inc., Wallingford CT, **2004**.
- [15] HyperChem(TM) Professional 8, Hypercube, Inc., 1115 NW 4th Street, Gainesville, Florida 32601, USA.
- [16] M. Freindorf, Y. Shao, T. R. Furlani, J. Kong, *J. Comput. Chem.* **2005**, 26, 1270.